

AEROBALLISTIC RANGE FACILITIES AND THEIR PERIPHERAL EQUIPMENT

AT LANGLEY RESEARCH CENTER

By John Di Battista  
NASA Langley Research Center  
Hampton, Virginia

This paper has been prepared for the Aeroballistic Range Association membership to provide a brief introduction to the ballistic facilities at Langley Research Center, and to indicate the general kinds of research that are currently being performed in the respective facilities.



— LANGLEY RESEARCH CENTER —

# AEROBALLISTIC RANGE FACILITIES AND THEIR PERIPHERAL EQUIPMENT

## AT LANGLEY RESEARCH CENTER

John Di Battista  
NASA Langley Research Center

Hampton, Virginia

This paper has been prepared to provide a brief introduction to the ballistic facilities at Langley Research Center, and to indicate the general kinds of research that are currently being performed in the respective LRC facilities.

There are four major ballistic facilities at LRC. These facilities are tabulated in Table 1, and they include various size light gas guns, a hailstone accelerator, an electrothermal and an electrostatic accelerator. With the exception of the hailstone accelerator, these facilities are being used to investigate meteoroid impact damage to spacecraft, to develop lightweight and low-cost meteoroid shielding devices, and to develop and calibrate flight instruments to measure the meteoroid environment in space. The hailstone accelerator is used principally to study hail damage to military aircraft and to civilian aircraft such as the supersonic transport.

The LRC facilities are capable of launching particles having a wide range of masses from  $1 \times 10^{-3}$  gram particles for the light gas guns down through  $1 \times 10^{-7}$  gram particles for the electrothermal accelerator to  $1 \times 10^{-16}$  gram particles for the electrostatic accelerator. However, it should be noted that although these accelerators can launch particles of widely different masses, only the electrothermal and electrostatic accelerators are capable of launching particles to even the low range of meteoroid velocities.

The remainder of this paper will describe each of the LRC facilities and their peripheral equipment.

I(a). 5.6 mm Pump Tube Light Gas Gun

Figures 1 and 2 are a schematic and photograph, respectively, of the LRC miniature light gas gun. The chief advantage of this gun is that it is inexpensive to operate, and it has a rapid firing rate of 8 to 10 times a day. The pump tube for the mini gun is a smooth-bore Swift rifle. The powder charge is contained in a standard 220 Swift rifle cartridge. A plastic bullet inserted in the cartridge serves as the piston to compress the hydrogen gas in the pump tube to high pressure for launch of the projectile. The projectile launching pressure is controlled by varying the thickness of a mylar diaphragm which is placed in the pump tube-launch tube coupling. During the final stage of the hydrogen gas compression cycle, the piston enters a tapered coupling section between the pump tube and launch tube and is swaged out through the launch tube to maintain the base pressure at a high value on the projectile. The barrels for this gun are commonly 25.4 cm long and 1.52 through 2.54 mm in diameter, and they are made of commercially available tubing.

Shown in figures 1 and 2 are the in-flight interrupted laser beam projectile detection station and projectile photographing system. The laser is a 1-milliwatt He-Ne laser, and the photomultiplier is a type 931-A. Spark gap light sources are used to back light the projectile so that image converter cameras can take 10 nanosec exposures. Figure 3 is a photograph of a 0.211-cm-diameter nylon sphere which was launched unsaboted to 7.0 km/s. The magnification for this photograph is 3.75. Even though unsaboted, the projectile remains spherical and undamaged.

Presently, this facility is being used to evaluate the effectiveness of a bumper protected main-wall configuration which will later be flight tested on the Meteoroid Technology Satellite. The facility is also being used to investigate the vulnerability of the Viking bioshield materials to meteoroid impact.

I(b). 19.0 mm Pump Tube Light Gas Gun

Figures 4 and 5 are a schematic and photograph, respectively, of the 19.0-mm pump tube light gas gun. This gun is also equipped with an interrupted laser light beam system to detect the projectile and synchronize a six-frame ultra-high-speed Beckman and Whitley image converter camera to photograph the model in flight or impacting a target. This ultra-high-speed camera is capable of taking 5 nanosec photographs at a framing rate of 200 million frames per second. Figure 6 presents a sequence of photographs taken with this camera showing a cylinder having a velocity of 7.0 km/s impacting a clear plastic block with a grid in a plane containing the projectile flight path. This gun is presently being used to study detailed impact phenomena.

I(c). 31.75 mm Pump Tube Light Gas Gun

Langley's newest light gas gun, a 31.75-mm pump tube gun, is shown in figures 7 and 8. This gun incorporates an Ames Research Center design high-pressure hydraulic coupling between the pump tube and launch tube. Whereas the previous 19-mm pump tube light gas gun is limited to launching sabot projectiles to velocities around 7 km/s, this gun is now being used to velocities of 8 km/s. An interrupted laser light beam projectile detection station is used along with image converter cameras to determine the projectile velocity and integrity. Also available for use on this gun are the

ultra-high-speed Beckman and Whitley six-frame image converter camera as shown in figures 7 and 8, and a continuous writing 80-frame high-speed framing camera which has a maximum framing rate of 1.4 million frames per second. This facility is used along with the previously described 19-mm pump tube light gas gun to study detailed impact phenomena.

## II Hailstone Accelerator

Figures 9 and 10 are a schematic and photograph, respectively, of the hailstone accelerator range. The accelerator launch tube diameter can be varied from 1.25 cm to 5.08 cm in diameter. The projectiles, which are ice spheres of the launch tube diameter, are accelerated by compressed air to velocities of 0.6 km/s or less. Higher velocities are possible by using helium as the driver gas. The entire launch tube and pump tube are cooled to 0° C before firing to prevent melting of the projectile. Either an interrupted laser beam or trip wire, which is strung across the particle flight path, is used to actuate a projectile photographic system. This system consists of two xenon filled flash lamps and two image converter cameras. As mentioned previously, this facility is being used to study hailstone damage to high-performance military and civilian aircraft; consequently, the ice projectiles here impact the targets in air.

Typical hail impact damage to thin 2024-T3 aluminum targets is shown in figure 11. The targets are a 0.10-cm-thick flat sheet (fig. 11(a)) and a 0.10-cm-thick spherical cap (fig. 11(b)) of radius 41 cm, and have been impacted by spherical hailstones 2.54 cm in diameter.

## III The Electrothermal Accelerator

In the electrothermal accelerator, projectiles are drag accelerated by expanding lithium gas. This gas is formed by vaporizing a

lithium wire with electrical energy discharged from a capacitor bank. The projectiles are glass spheres on the order of 50 to 100 microns in diameter. Figure 12 is a schematic of the facility which shows the relative position of the capacitor bank, the exploding lithium wire gun, the evacuated range impact chambers, and the control panel. Figure 13 is a photograph of the capacitor bank which consists of 11 2.2 $\mu$ f, 60,000-volt capacitors each of which stores a maximum of 3960 joules. Also shown in figure 13 is the position of the exploding lithium wire gun and projectiles. Figure 14 is a photograph of the housing for the exploding lithium wire gun and projectiles. Figure 15 is a photograph of the evacuated test range where the targets are located. Also shown in figure 15 is a Beta-graph unit which is capable of taking 2-nanosec exposures. Figure 16 is a plot which shows the velocity for loaded 50-micron-diameter glass projectiles versus discharge voltage of the capacitor bank.

The electrothermal accelerator is presently being used to impact bumper-protected targets of the type to be flown on the Meteoroid Technology Satellite and to test the meteoroid velocity sensors which will also be flown on the same satellite. The accelerator is also being used to test meteoroid penetration detectors which will be placed on Pioneer F and G spacecraft for flights through the asteroid belt and out to Jupiter.

#### IV The Electrostatic Accelerator

Figure 17 is a schematic of the LRC electrostatic accelerator facility showing the relative position of the Van de Graaff, the in-flight particle diagnostic instrumentation, and the impact chambers. In this facility carbonyl iron particles are used as projectiles. Figure 18 is a photograph showing the 4-million-volt Van de Graaff accelerator column.

The iron particles are charged and released from the particle charge injector. These particles are subsequently accelerated through the electric field setup in the accelerator tube. Figure 19 shows three projectile detection stations used in determining the particle velocity. To control the velocity of particles which are to impact a given target, a particle rejection station is used to exclude any particle not having the correct velocity. Particle rejection is accomplished by activating an electric field which deflects the charged particle to a flight path such that it fails to impact the target. Figure 20 shows the terminal impact chambers used to study erosion damage on shiny surfaces, and also a luminosity chamber to study particle radiation occurring during high-speed passage through a gas.

The accelerator, although most commonly used in studies which require a great number of particle impacts, does have single shot capability. In addition, the velocity and mass for each particle impacting a target is recorded automatically on magnetic tape. Quantities such as incident momentum and energy, and particle mass and velocity distributions are instantly available. The last figure, figure 21, shows the particle velocity versus particle size capability for this accelerator.

Presently, this accelerator is being used to study erosion damage to the orbiting 3-meter-diameter telescope mirror, impact response of silicon-oxide meteoroid detection sensors, and the meteoroid velocity sensor to be flown on the Meteoroid Technology Satellite.

Table 1

Particle Accelerators at Langley Research Center

- I. Light gas guns
  - (a) 5.6 mm pump tube with 1.5 mm through 2.5 mm barrels
  - (b) 19.0 mm pump tube with 5.6 mm and 7.6 mm barrels
  - (c) 31.75 mm pump tube with 5.6 mm and 7.6 mm barrels
  
- II. Hailstone accelerator
  
- III. Electrothermal accelerator
  
- IV. Electrostatic accelerator



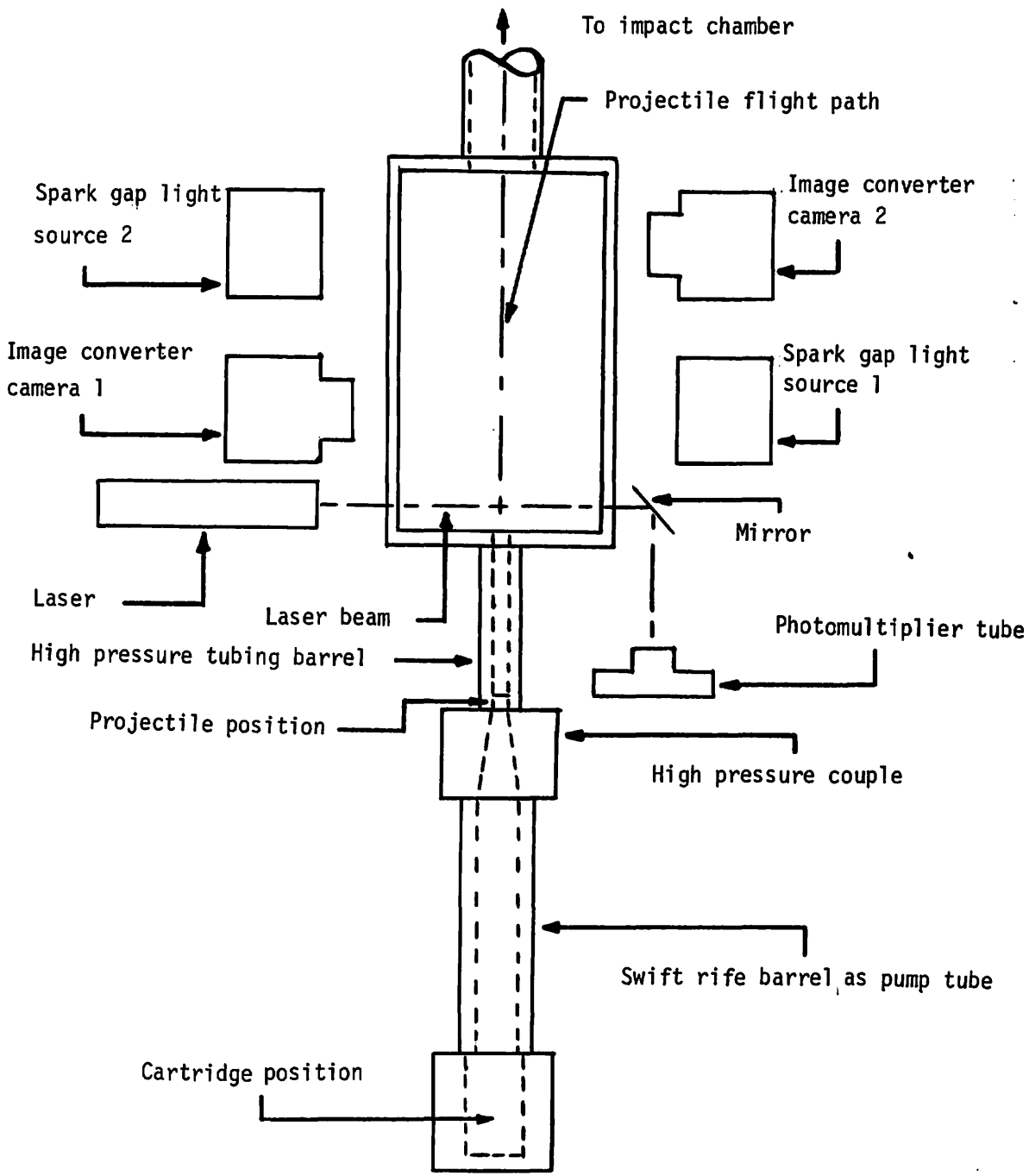


Figure 1.- Schematic of 5.5-mm-diam pump tube light gas gun range.

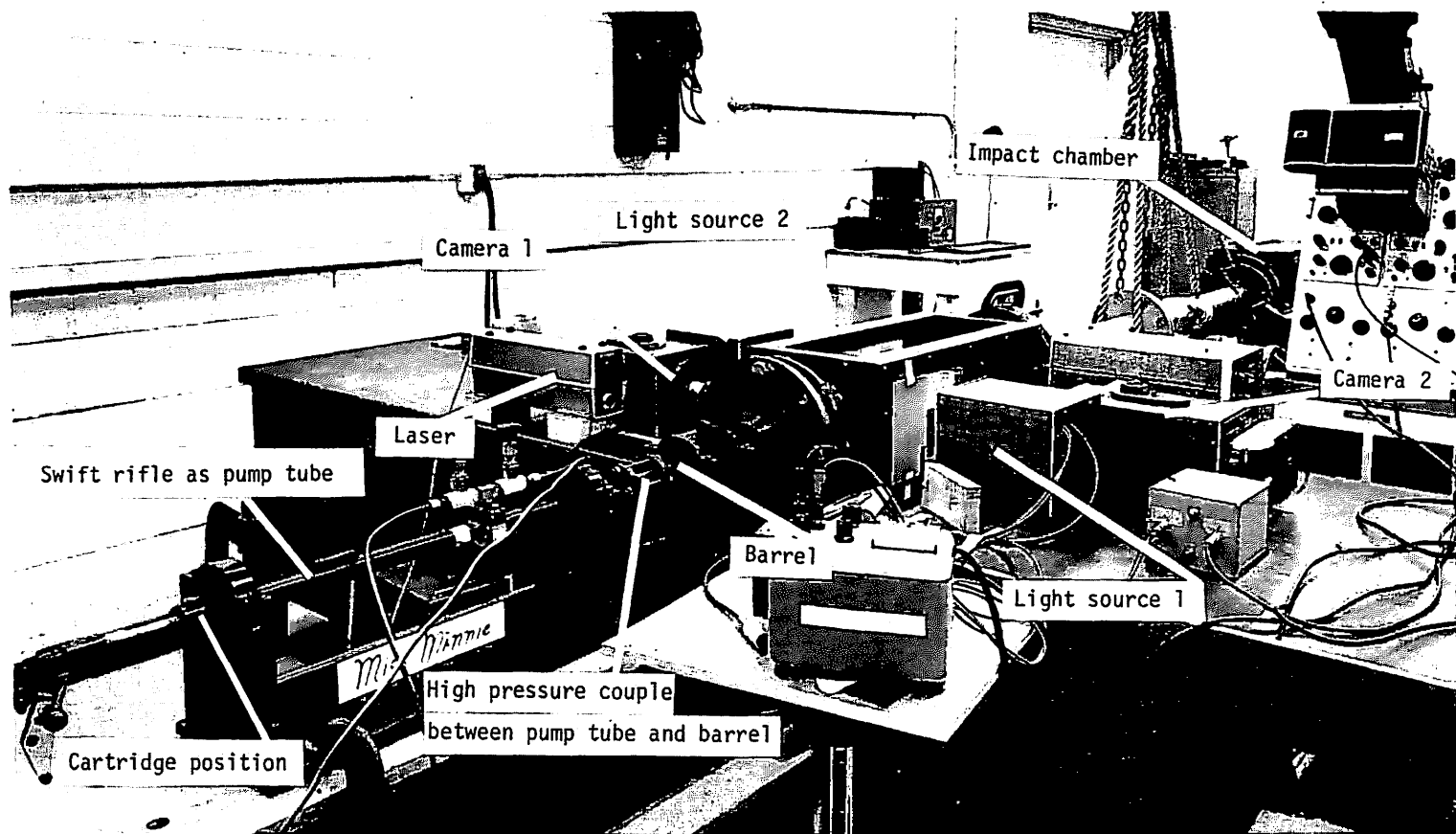


Figure 2.- 5.5-mm-diam pump tube light gas gun.

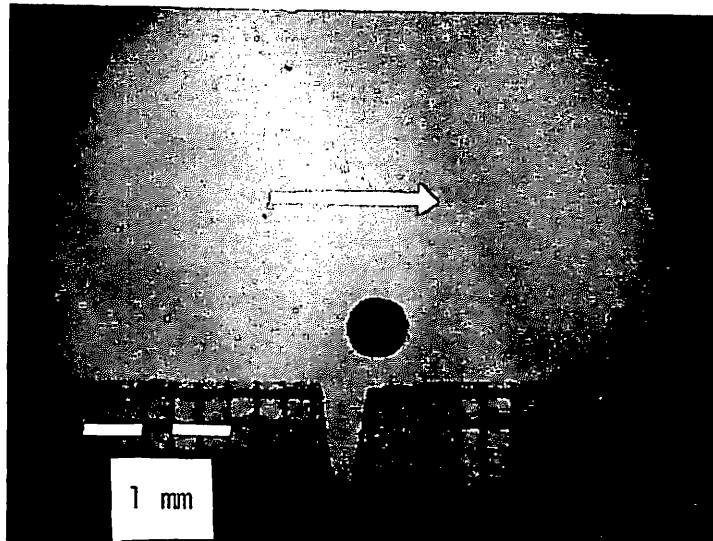


Figure 3.- In-flight photograph of a 0.211-cm-diam nylon sphere having velocity of 7 km/s. The magnification of the sphere is 3.75.

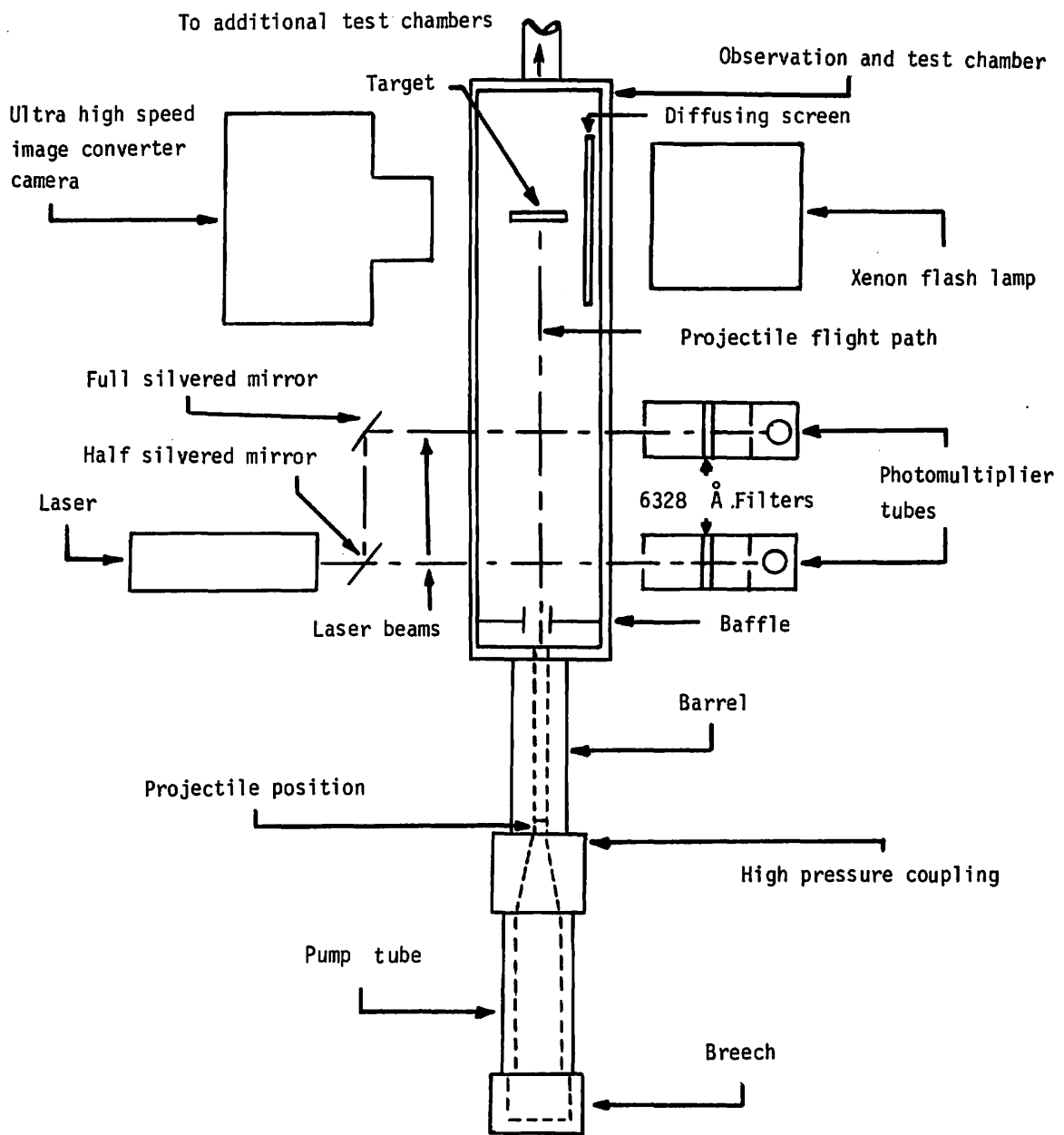


Figure 4.- Schematic of 19-mm-diam pump tube light gas gun range.

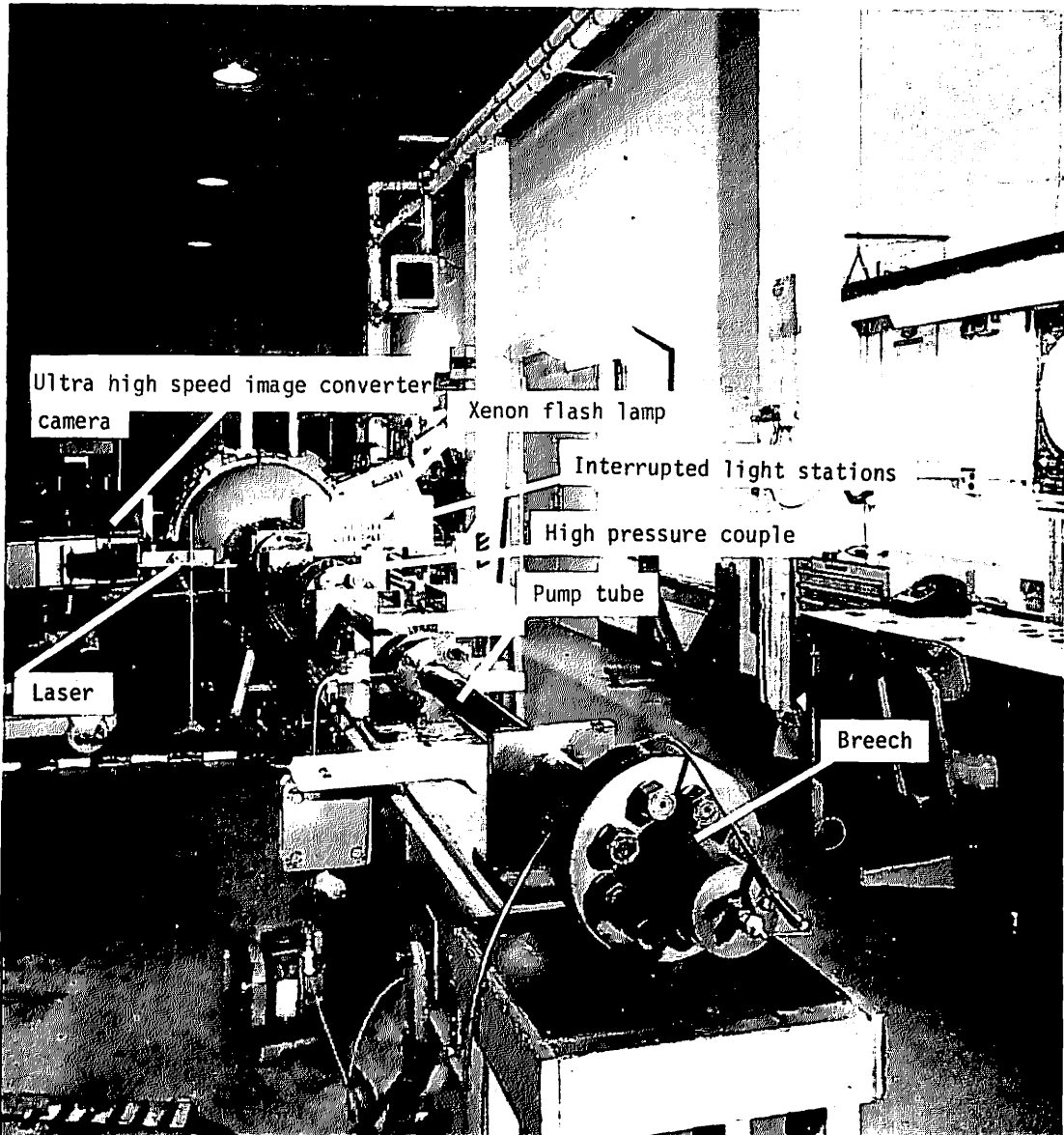
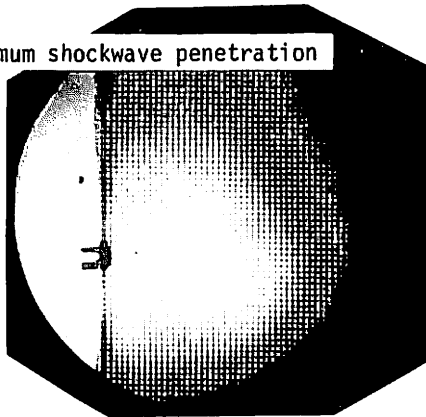


Figure 5.- View from breech end of 19-mm-diam pump tube light gas gun.

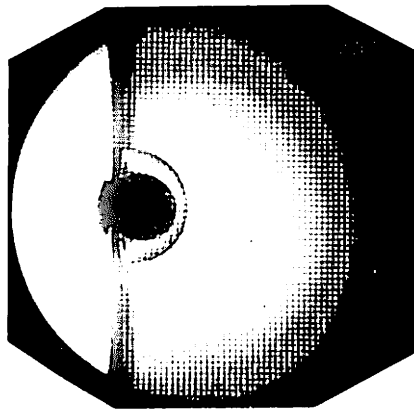
t = time

d = maximum shockwave penetration



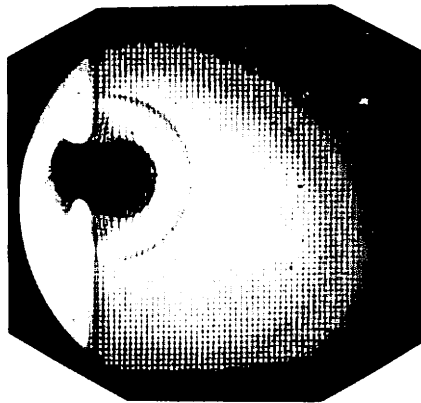
t = 0.0  $\mu$  sec      d = .99 mm

(a)



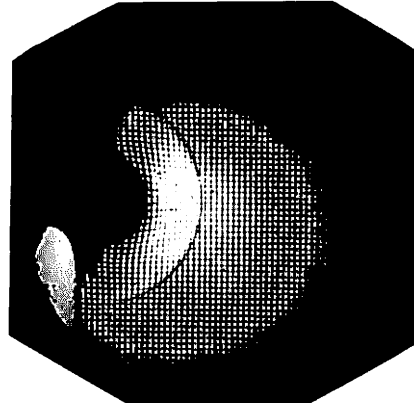
t = 2.78  $\mu$  sec      d = 14.80 mm

(b)



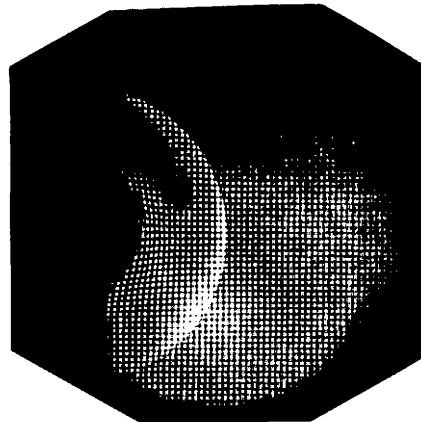
t = 4.59  $\mu$  sec      d = 21.59 mm

(c)



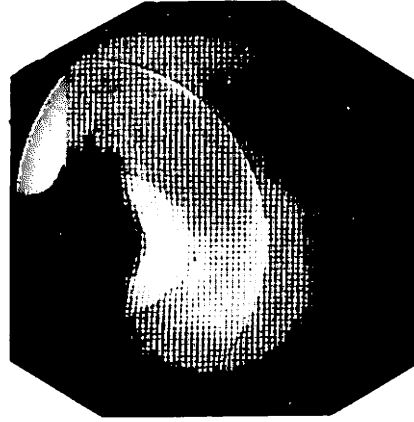
t = 6.38  $\mu$  sec      d = 27.24 mm

(d)



t = 9.30  $\mu$  sec      d = 36.29 mm

(e)



t = 12.01  $\mu$  sec      d = 44.76 mm

(f)

Figure 6.- 7 km/s impact of a polycarbonate cylinder, 0.564 cm in diameter and 0.782 cm in length, into a methyl-methacrylate target having a 0.127-cm by 0.127-cm grid in the projectile flight path.

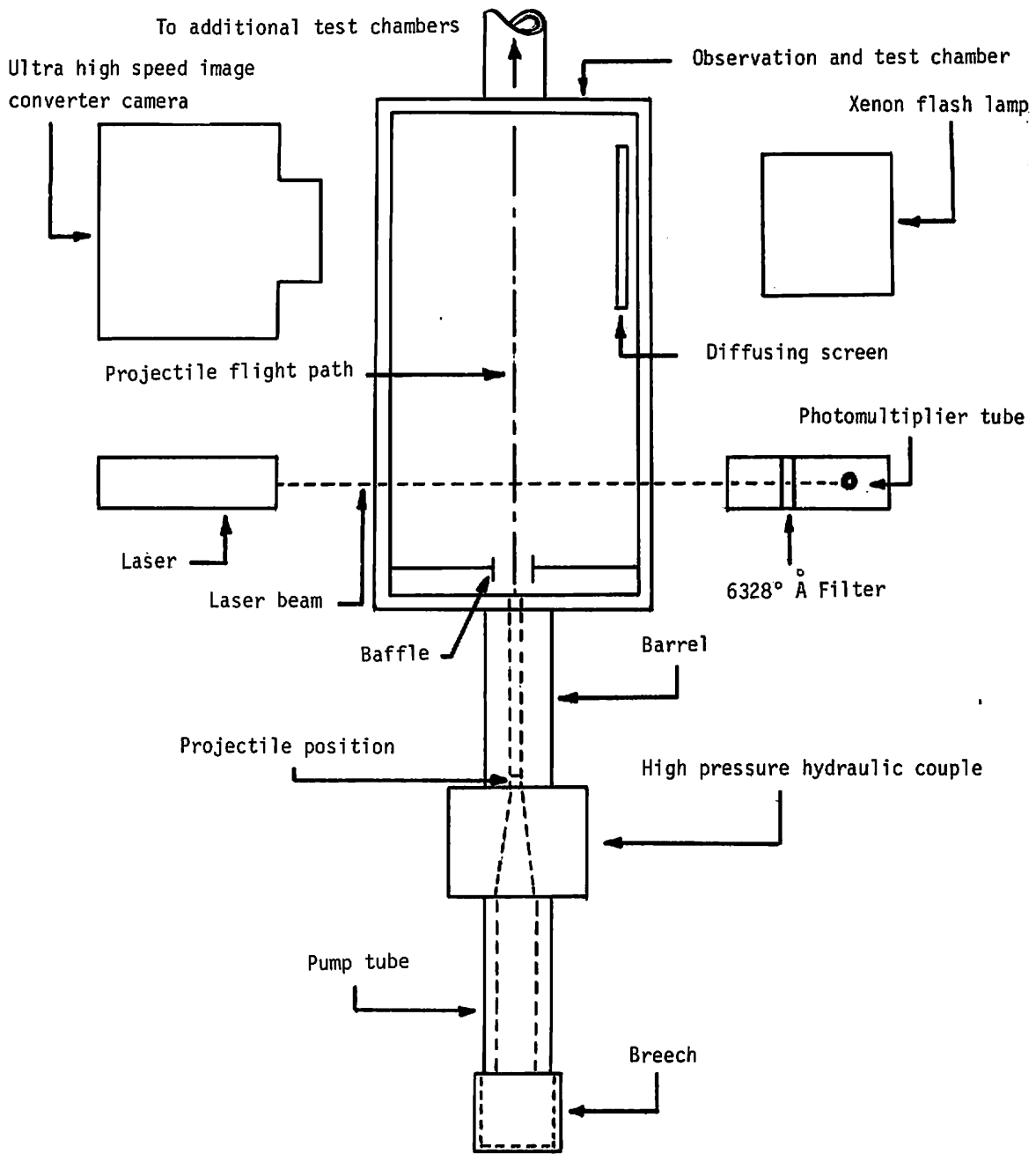


Figure 7.- Schematic of 31.75-mm-diam pump tube light gas gun range.

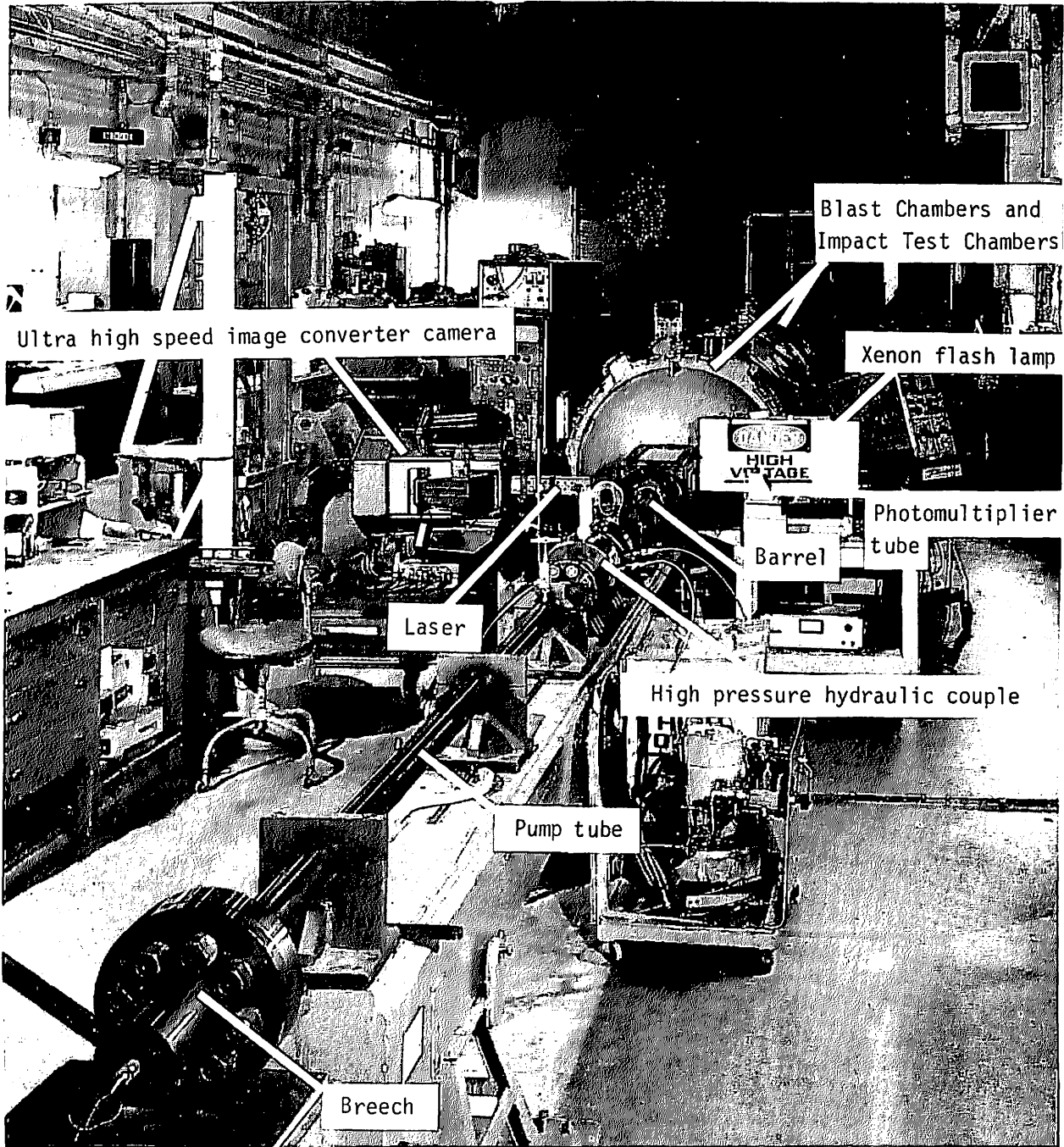


Figure 8.- View from breech end of 31.75-mm-diam pump tube light gas gun.



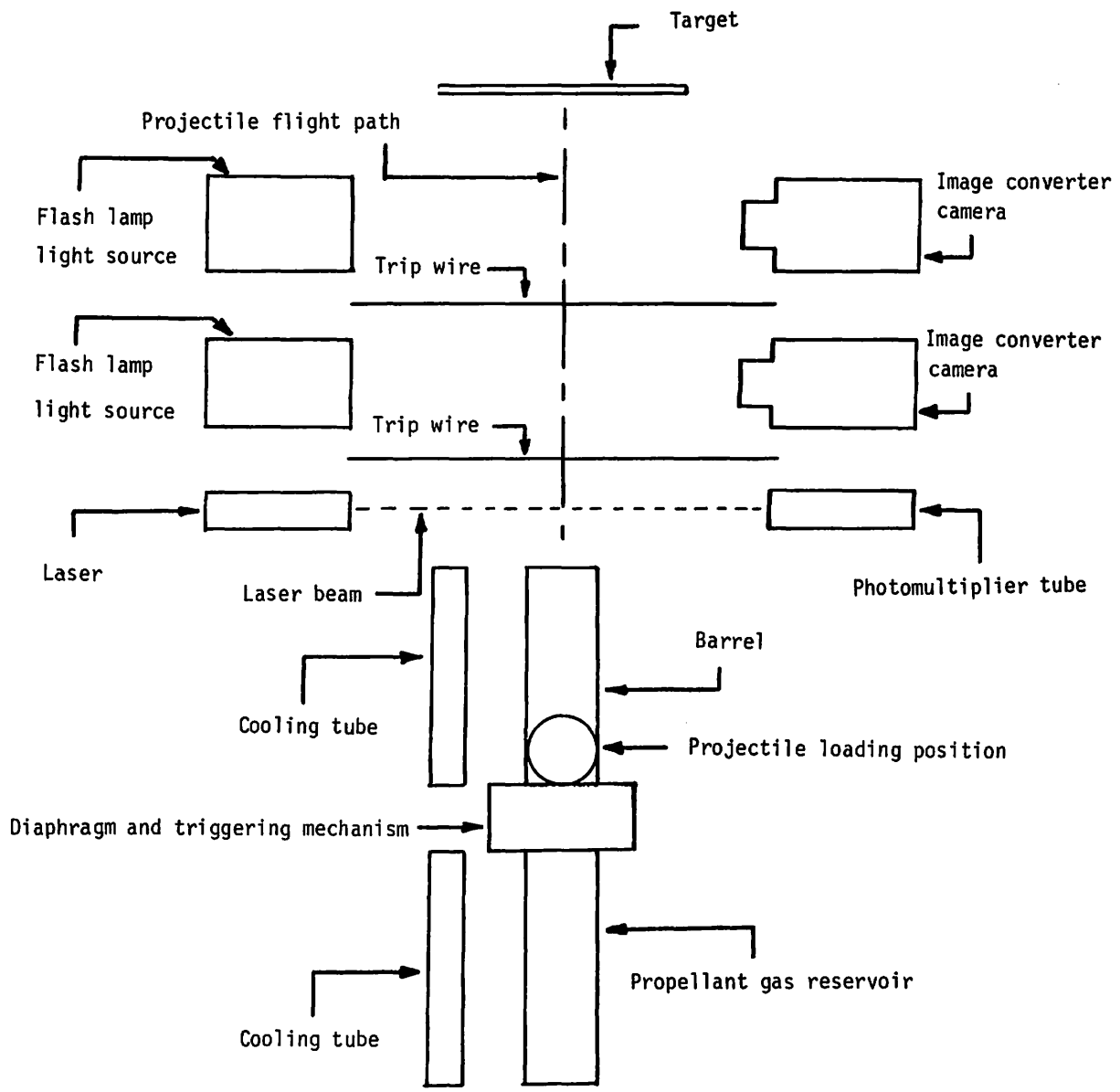


Figure 9.- Schematic of hailstone accelerator range.

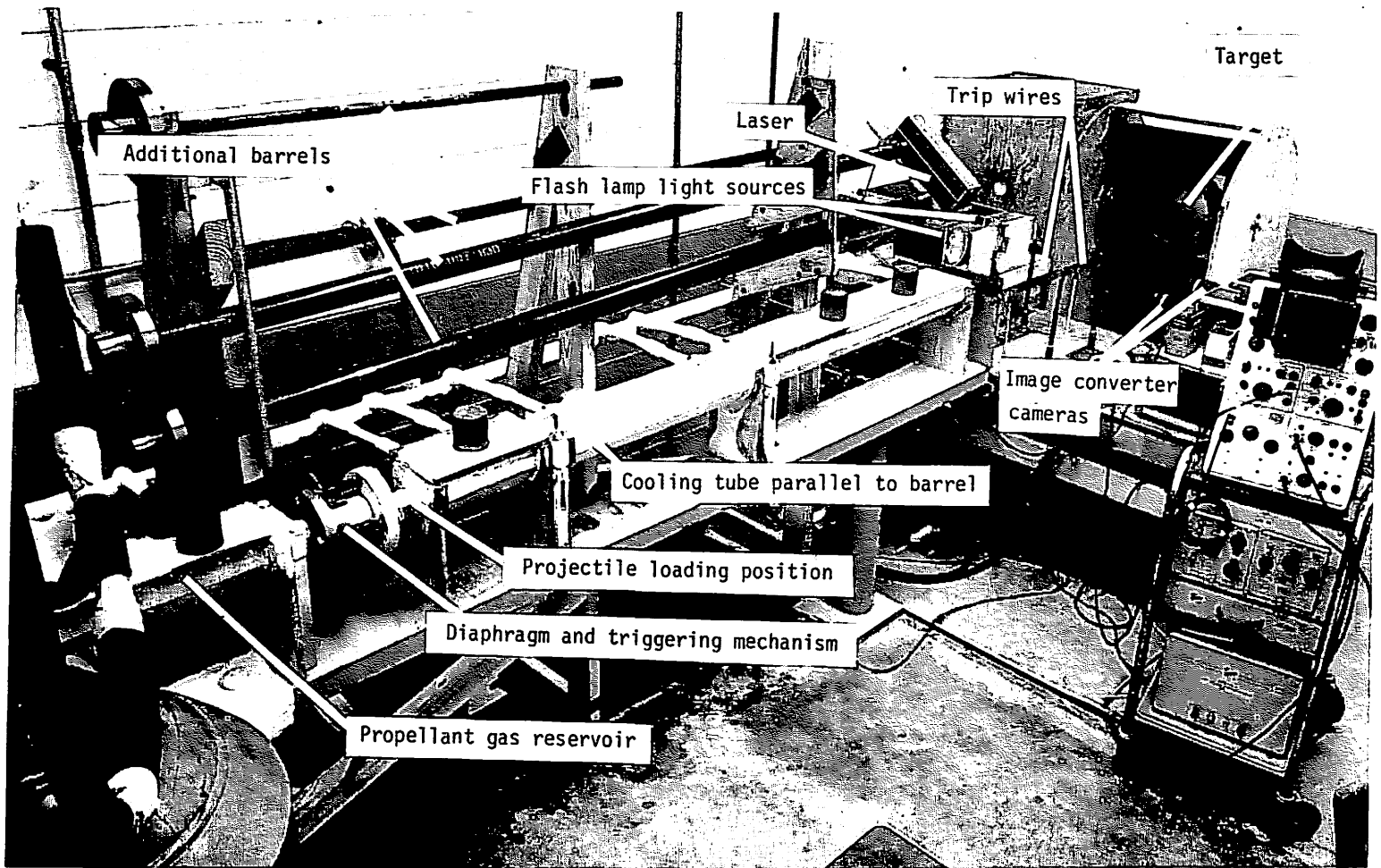
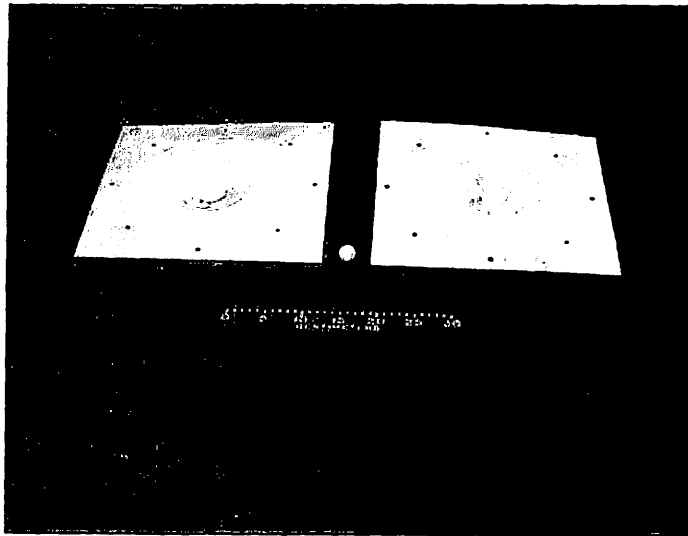
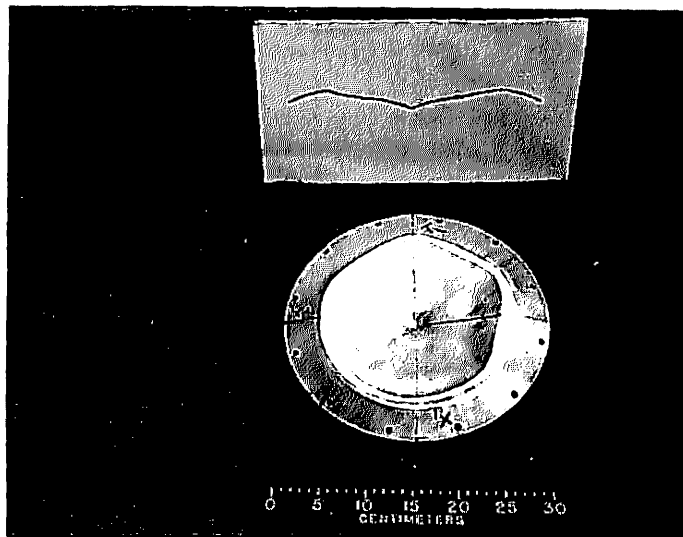


Figure 10.- Hailstone accelerator range.

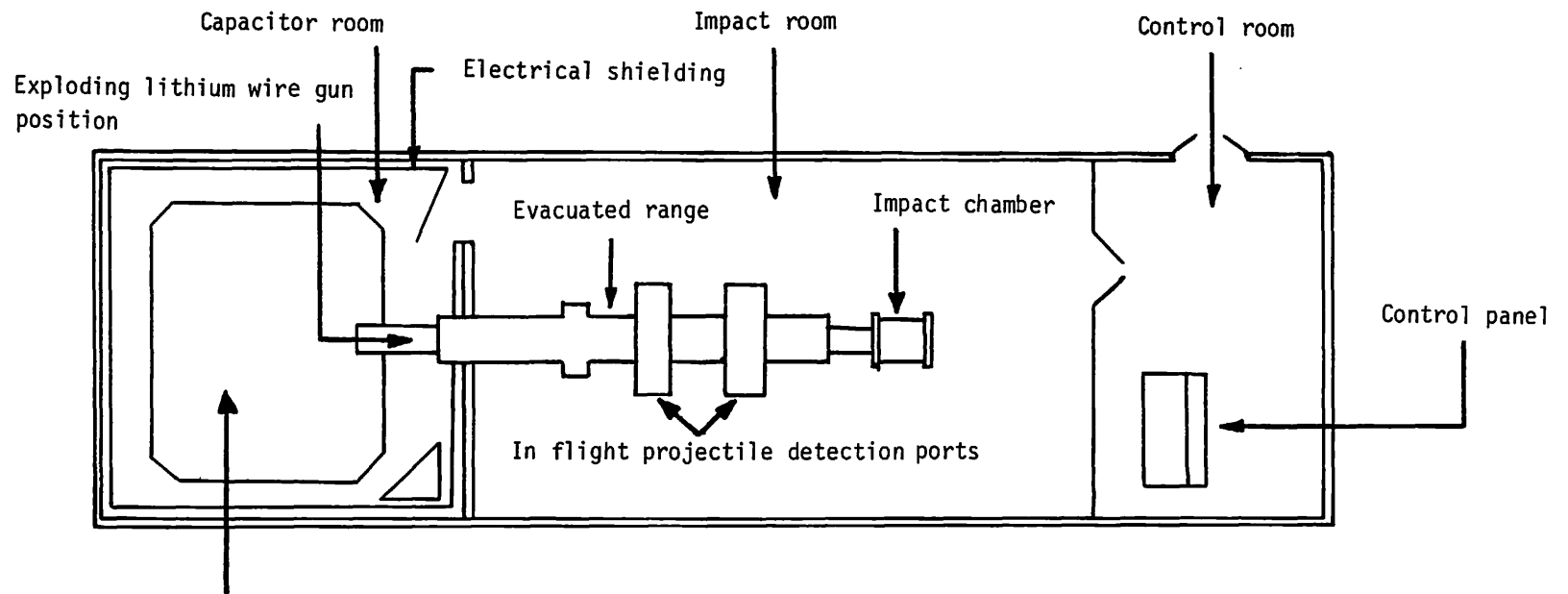


(a) Flat sheet; impact velocity 0.37 km/s.



(b) Spherical cap; impact velocity 0.25 km/s.

Figure 11.- Normal impact of 2.54-cm-diam hailstones into 0.1-cm-thick aluminum targets.



Capacitor bank composed of eleven  $2.2 \mu f$ , 60,000 volt capacitors each with a maximum stored energy of 3960 joules.

Figure 12.- Schematic of electrothermal accelerator facility.

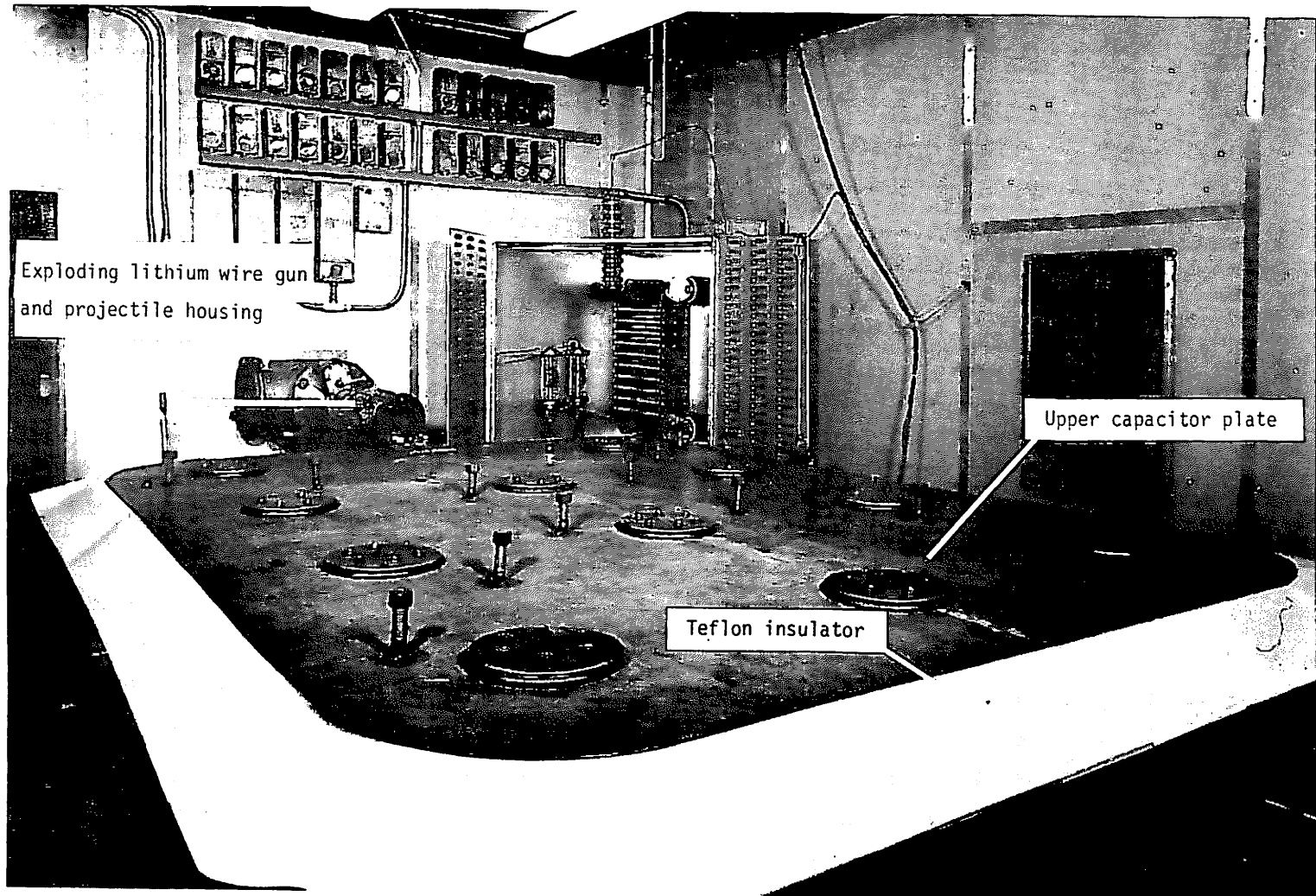


Figure 13.- Electrothermal capacitor bank.

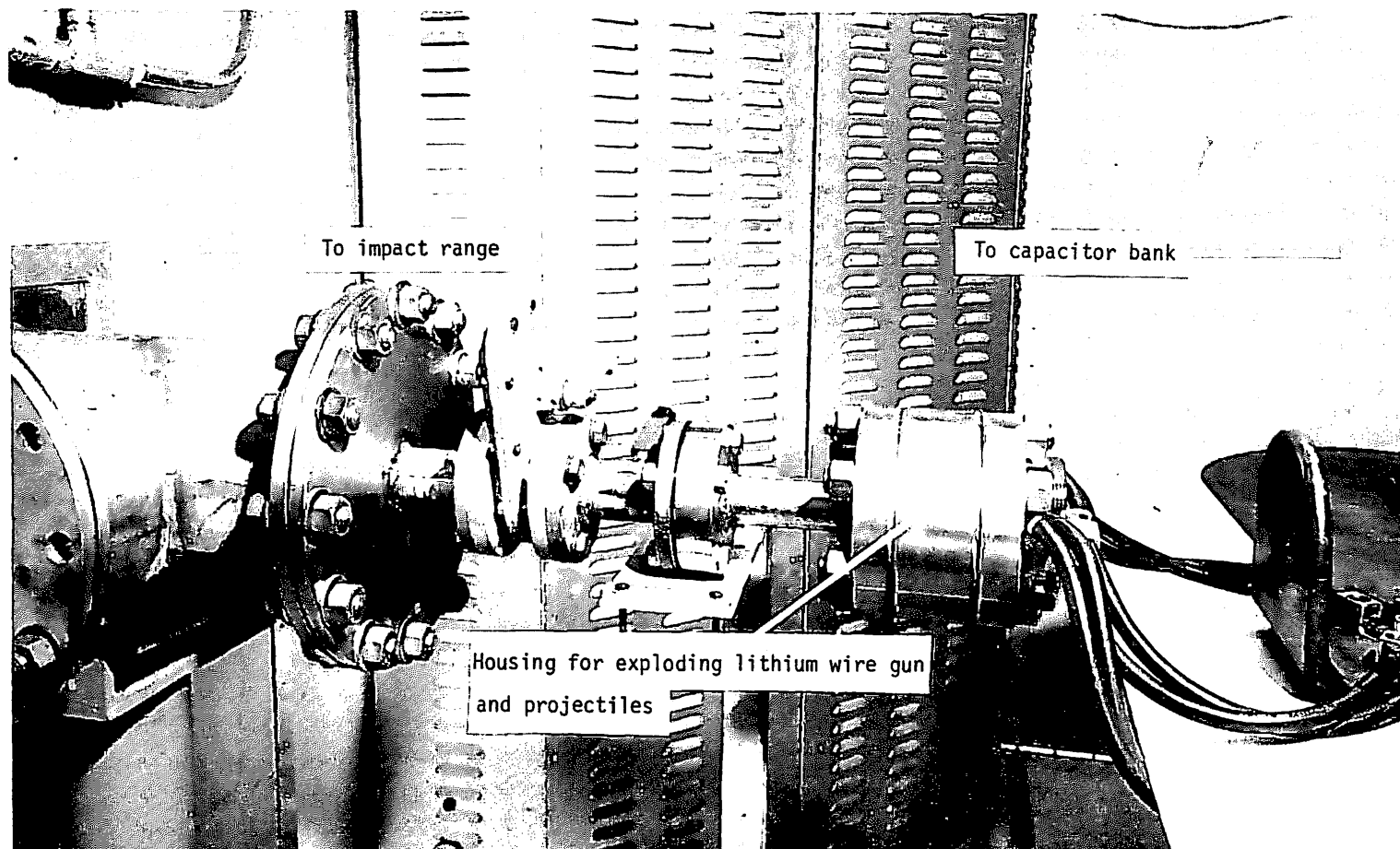


Figure 14.- External view of exploding lithium wire gun and projectile housing.

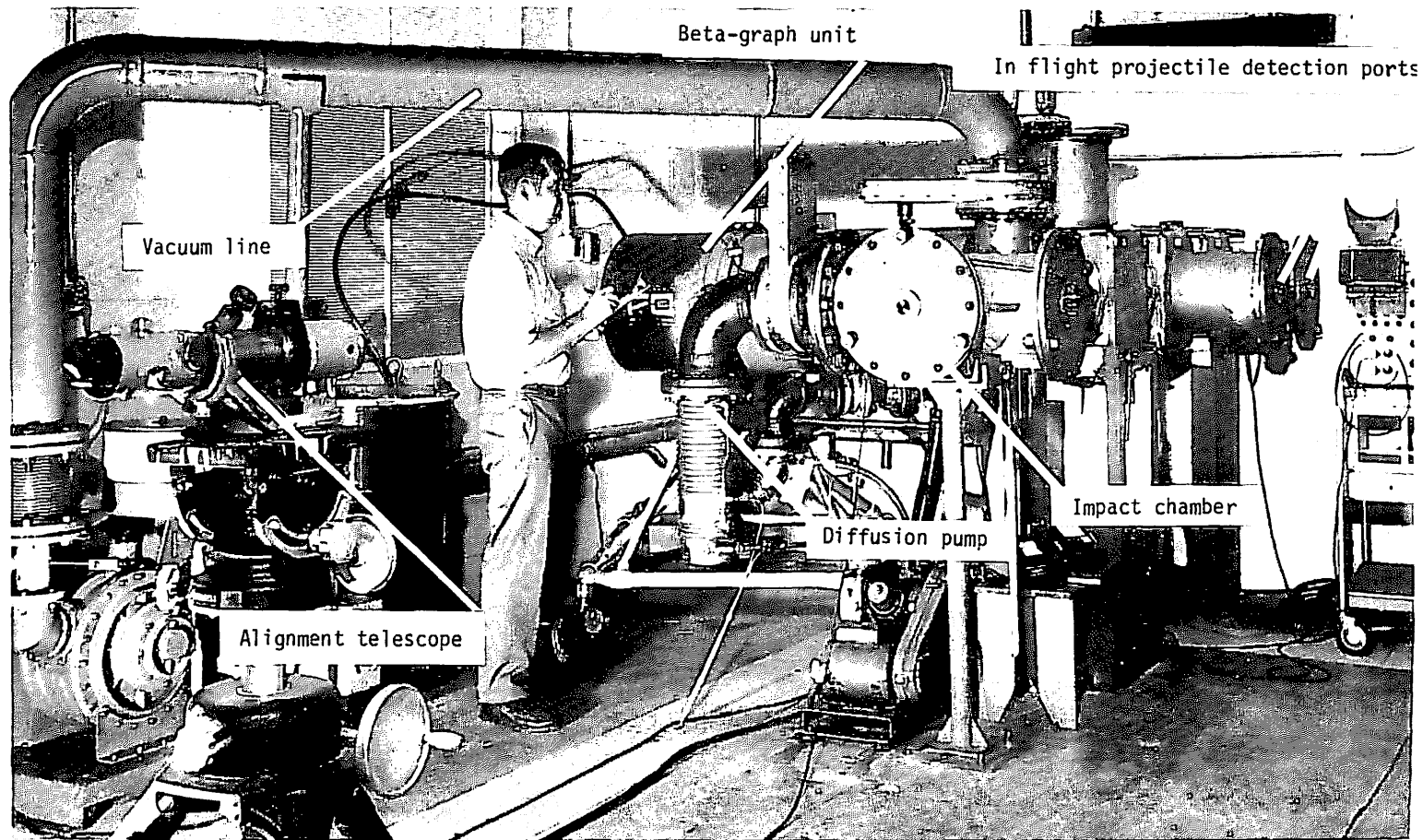


Figure 15.- Impact room of electrothermal accelerator facility.

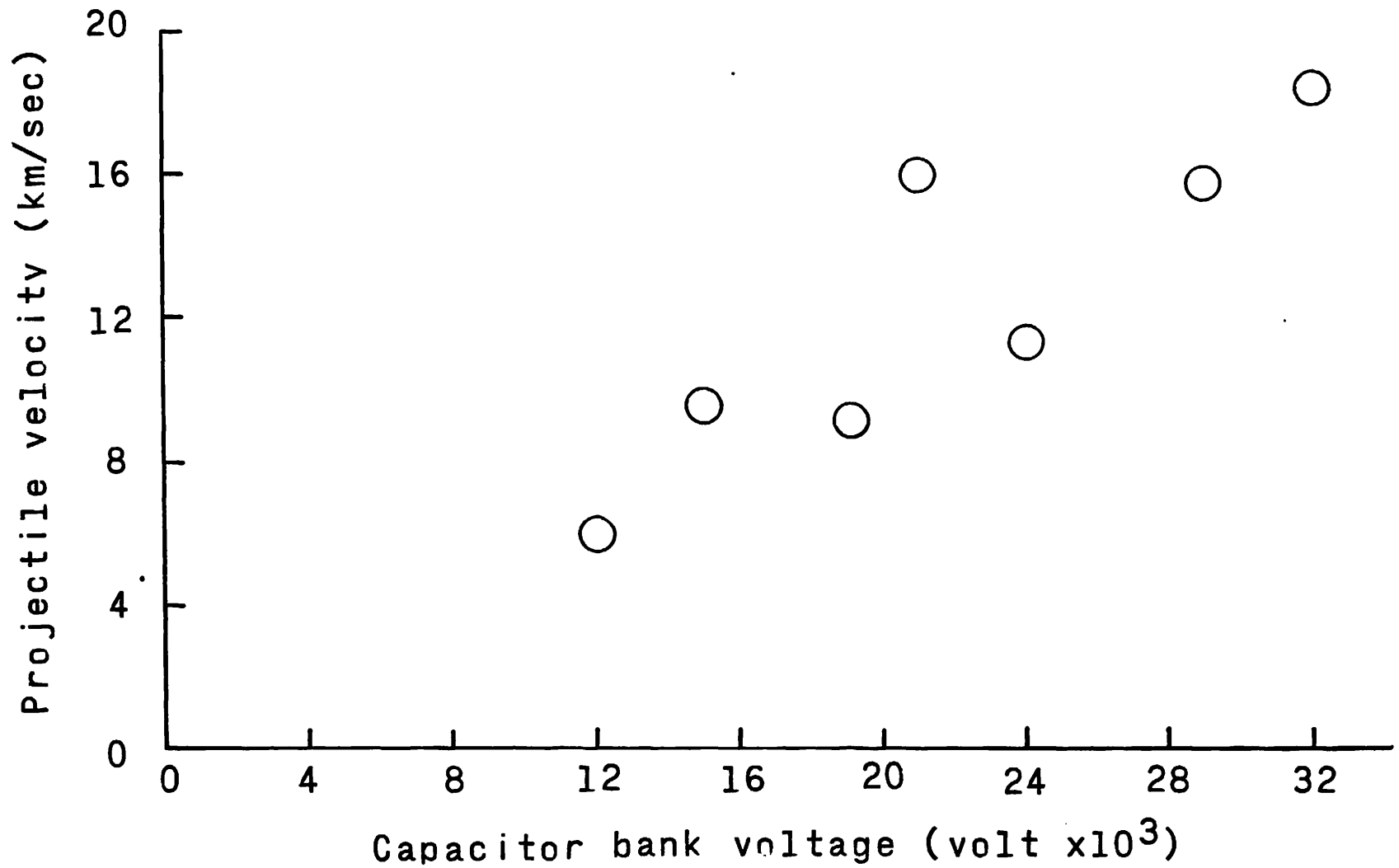
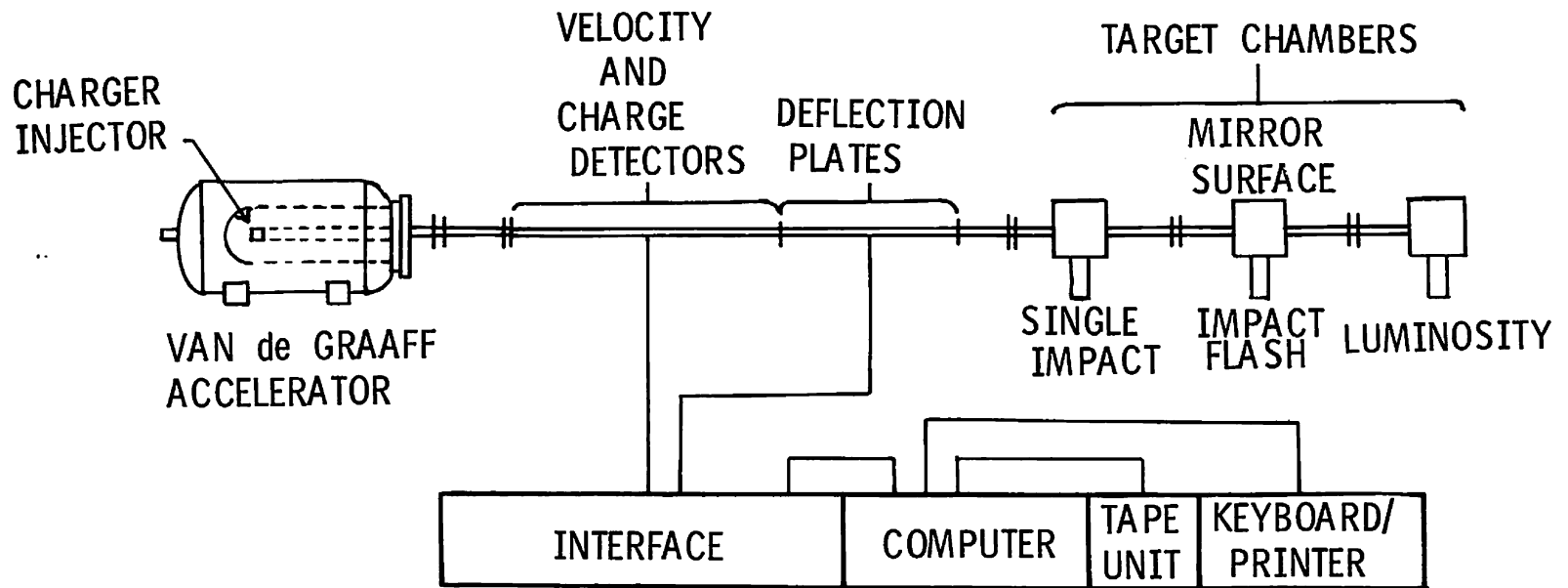


Figure 16.- Velocity of 50-micron-diam glass spheres with various capacitor bank voltages.





### DATA ACQUISITION SYSTEM PERFORMANCE CHARACTERISTICS

CARBONYL IRON PARTICLES; DENSITY  $7.86 \times 10^3 \text{ kg/m}^3$

PARTICLE DIAMETER RANGE; .1 to 10  $\mu\text{m}$

PARTICLE RATES TO GREATER THAN 10/s

PARTICLE VELOCITY RANGE;  $1 < v < 35 \text{ km/s}$

MEASURES AND RECORDS PARTICLE PARAMETERS

Figure 17.- Schematic of electrostatic accelerator range.

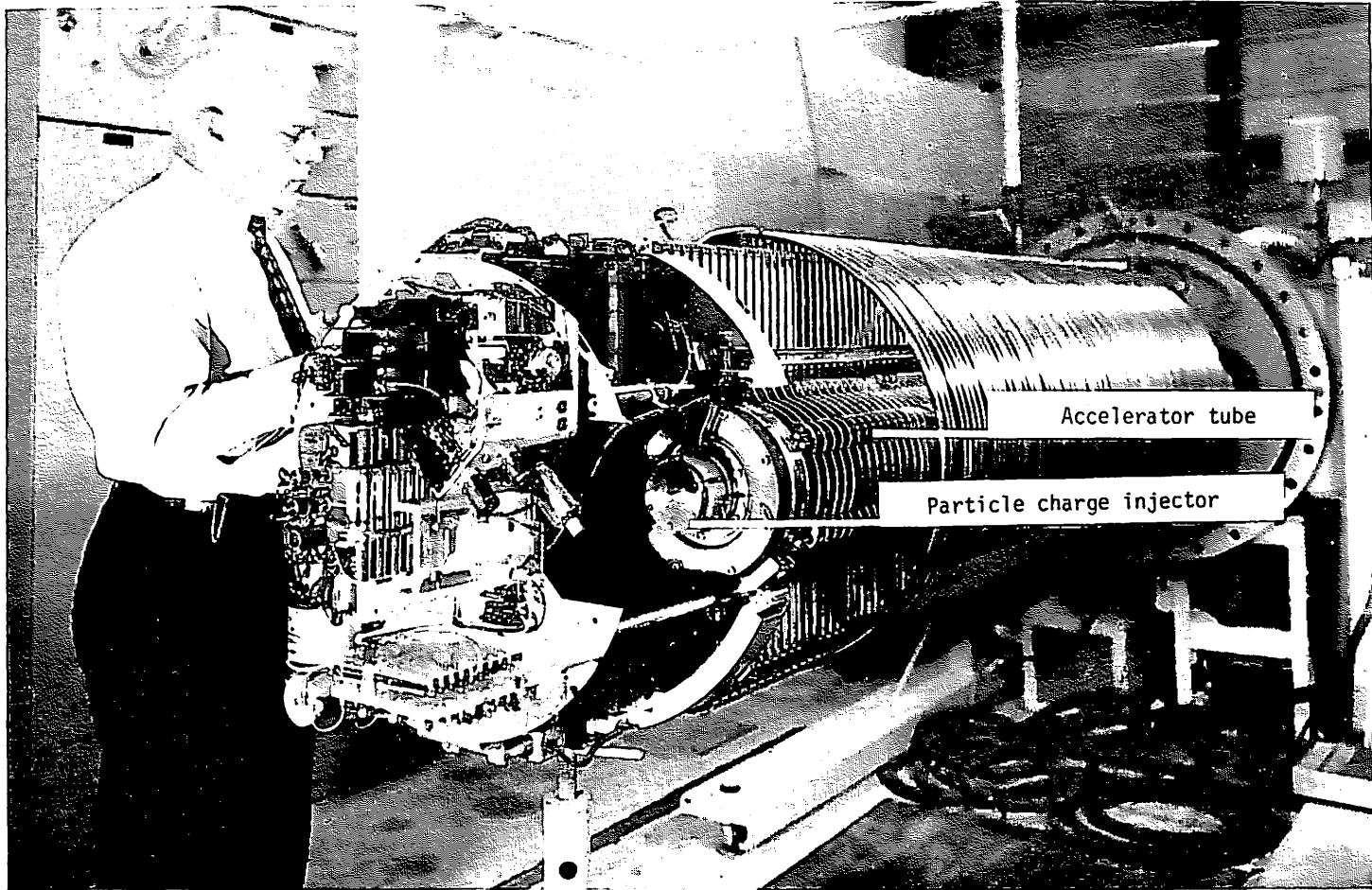


Figure 18.- Van de Graaff accelerator column.

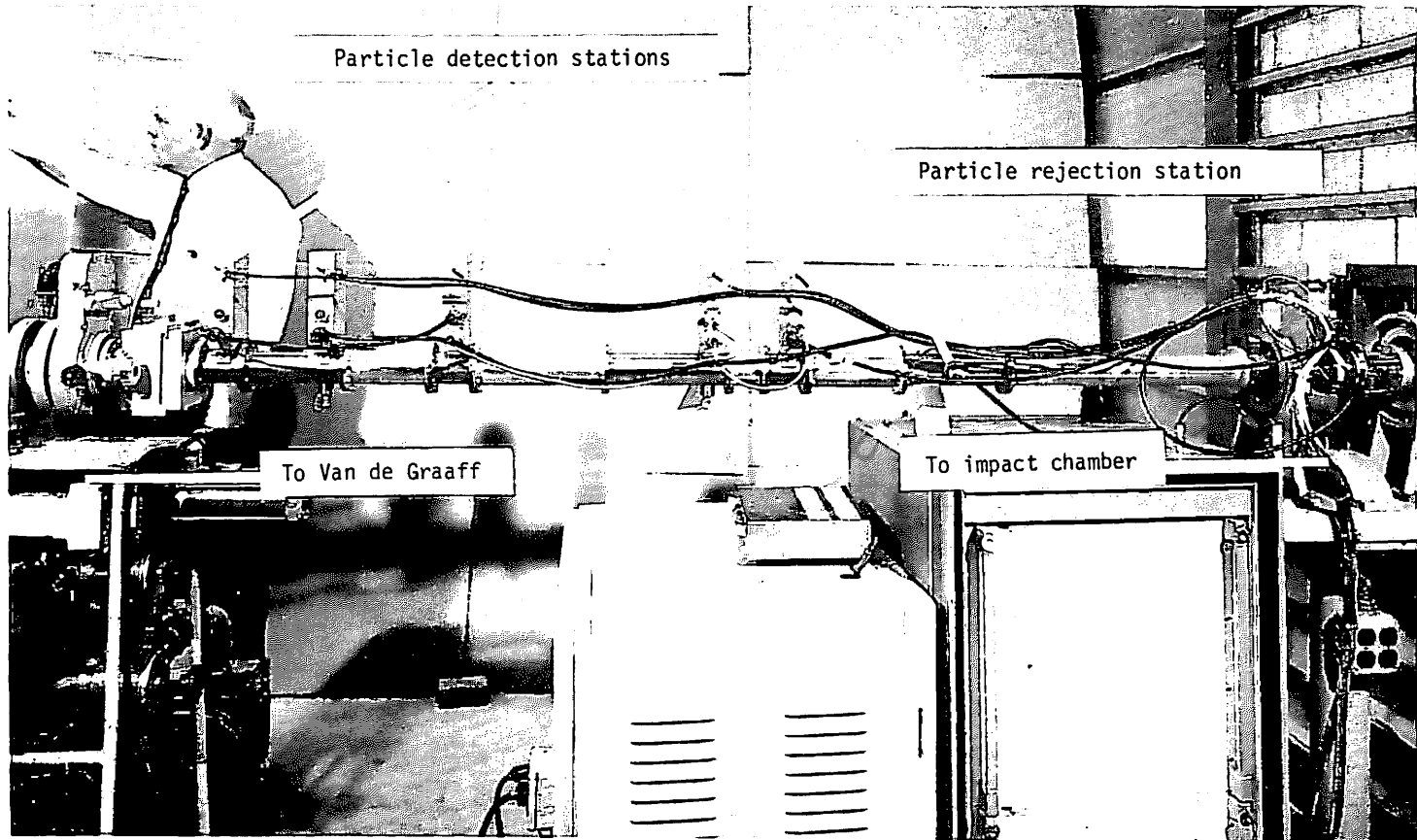


Figure 19.- Particle detection and rejection stations.

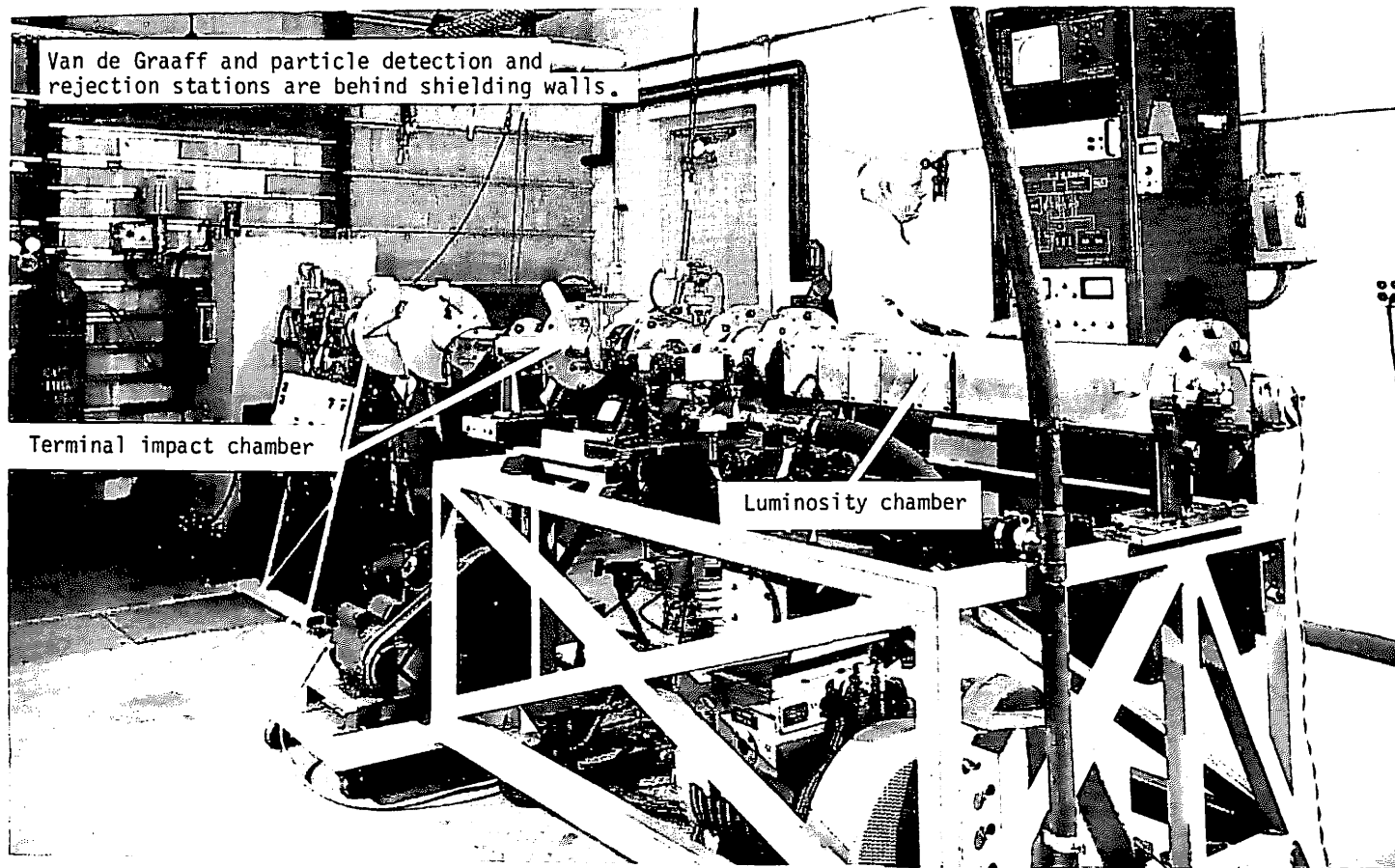


Figure 20.- Impact chambers.

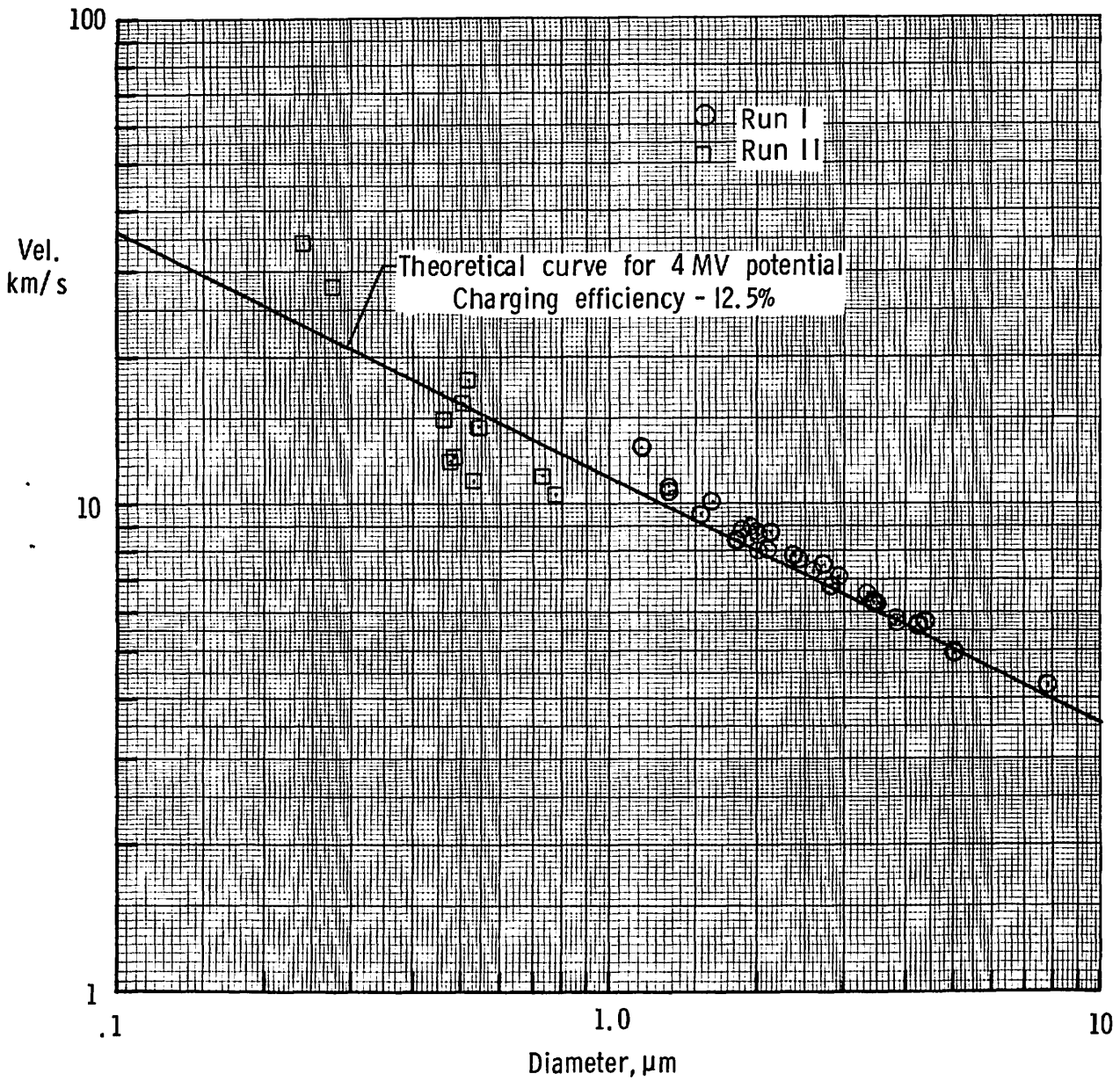


Figure 21.- Variation of microparticle velocity with diameter for 4-million-volt potential.